

Complete Structure of the Anti Rotamer of 1,2-Difluoroethane from High-Resolution Infrared Spectroscopy

Norman C. Craig,* Anthony Chen, and Ki Hwan Suh

Department of Chemistry, Oberlin College, Oberlin, Ohio 44074

Stefan Klee, Georg C. Mellau, Brenda P. Winnewisser, and Manfred Winnewisser

Physikalisch-Chemisches-Institut der Justus-Liebig-Universität, D-35392 Giessen, Germany

Received: August 19, 1997; In Final Form: October 1, 1997[⊗]

B-type bands in the high-resolution, gas-phase infrared spectra of two isotopomers of 1,2-difluoroethane have been recorded and analyzed in detail. These bands are due to the in-plane, antisymmetric CCF bending fundamental (ν_{18}) of the low-abundance anti rotamer of the d_4 and $^{13}C_2$ species and are centered at 264.257 and 279.410 cm^{-1} , respectively. Watson-type rotational Hamiltonians have been fit to the ground state (GS) and excited vibrational state for each molecule. A complete structure for the anti rotamer has been derived from the GS rotational constants of these two isotopomers and the previously reported normal species. The r_0 values are $r_{CH} = 1.092$ Å, $r_{CC} = 1.506$ Å, $r_{CF} = 1.400$ Å, $\alpha_{CCH} = 111.6^\circ$, $\alpha_{HCH} = 110.7^\circ$, $\alpha_{CCF} = 107.3^\circ$, and $\alpha_{FCH} = 107.8^\circ$. These geometric parameters are compared with those of the gauche rotamer and together with values for both rotamers from ab initio calculations. The changes in the parameters between the two rotamers are discussed in relation to the gauche effect, the surprisingly lower electronic energy of the polar gauche rotamer.

Introduction

The two rotamers of 1,2-difluoroethane (DFEA) have an exceptional energy relationship. The polar rotamer with proximate CF bonds has a lower electronic energy than the nonpolar anti rotamer by 2.4–3.4 kJ/mol.^{1,2} This unusual energy relationship is known as the gauche effect.³ The gauche effect is also observed for the rotamers of 1,2-dimethoxyethane and for the rotamers of ethylene glycol.⁴ In the latter case hydrogen bonding may, however, play a role. A corresponding cis effect exists in the energy relationship of the isomers of 1,2-difluoroethylene, 1,2-difluorodiazene, and several other halogen- and oxygen-substituted ethylenes.⁵ For these ethylenes the cis isomer has the lower energy.

Through ab initio calculations, Wiberg and co-workers have recently investigated the gauche and cis effects in depth.⁶ Dixon and Smart have also done a range of ab initio calculations on these effects.⁷ Other investigators have done extensive ab initio calculations to compare the cis and trans isomers of 1,2-difluoroethylene, as summarized before.⁸ Durig, Liu, Little, and Kalasinsky also report ab initio calculations on the two rotamers of DFEA.² Muir and Baker have compared the results of calculating energies and geometric parameters with the adiabatic connection method (ACM) and various semiempirical and other ab initio methods for a number of fluorocarbons including the two rotamers of DFEA and the two isomers of 1,2-difluoroethylene.⁹

Wiberg has explained the gauche and cis effects in terms of a difference in bent bond contributions to the σ part of the CC bond that destabilizes the anti or trans species relative to the corresponding gauche or cis species. According to this model, the highly electronegative fluorine atom causes an increased p character in the C–F bond and thus a reduced angle between the carbon orbitals pointing toward the other carbon atom and the fluorine atom. Repulsion between the nonbonded atoms on each side of the CC bond causes tilting of the carbon orbitals away from the C–C axis. This tilting gives a more unfavorable

overlap for the σ part of the CC bond for the anti or trans configuration than for the corresponding gauche or cis one. Wiberg and co-workers used differences in electron density plots at two levels of theory in support of this bent bond interpretation.

Epiotis has used qualitative valence bond arguments to rationalize the difference in adjustments of bond lengths for the two rotamers of DFEA in comparison with the two isomers of 1,2-difluoroethylene.¹⁰ He anticipates an increase in both the CC and CF bond lengths in going from the gauche to the anti rotamer of DFEA in contrast to a decrease in the CC bond length but an increase in the CF bond length in going from the cis to the trans isomer of 1,2-difluoroethylene.

Important contributions to the investigation of the gauche and cis effects are experimentally well-based structures for both members of rotameric and isomeric pairs. In general, good structural information exists for the polar gauche and cis species from microwave spectroscopy. Takeo, Matsumura, and Morino have obtained a complete structure for the gauche rotamer of DFEA by this method.¹¹ Until recently, incomplete information has been available, at best, for nonpolar trans and anti species. Lacking dipole moments, these latter species are not amenable to investigation by pure rotational spectroscopy in the microwave region. For the anti rotamer of DFEA an electron diffraction study yielded no information^{12,13} because the gauche rotamer is 85% or more abundant at room temperature. At lower temperature the dominance by the lower energy gauche rotamer is even greater. At high temperature the anti rotamer is at best about 33% of the mixture.

High-resolution infrared spectroscopy provides access to the complete structures of nonpolar molecules of modest size. This method has recently been applied to the trans isomer of 1,2-difluoroethylene.¹⁴ We now report a complete, largely substitution structure for the anti rotamer of DFEA obtained by the infrared method.¹⁵

Despite the dominance of the infrared spectrum of DFEA by the gauche rotamer, one band in the spectrum is due almost entirely to the anti rotamer. This is the fundamental band, which arises from ν_{18} (b_u symmetry species), the largely antisymmetric

[⊗] Abstract published in *Advance ACS Abstracts*, November 15, 1997.

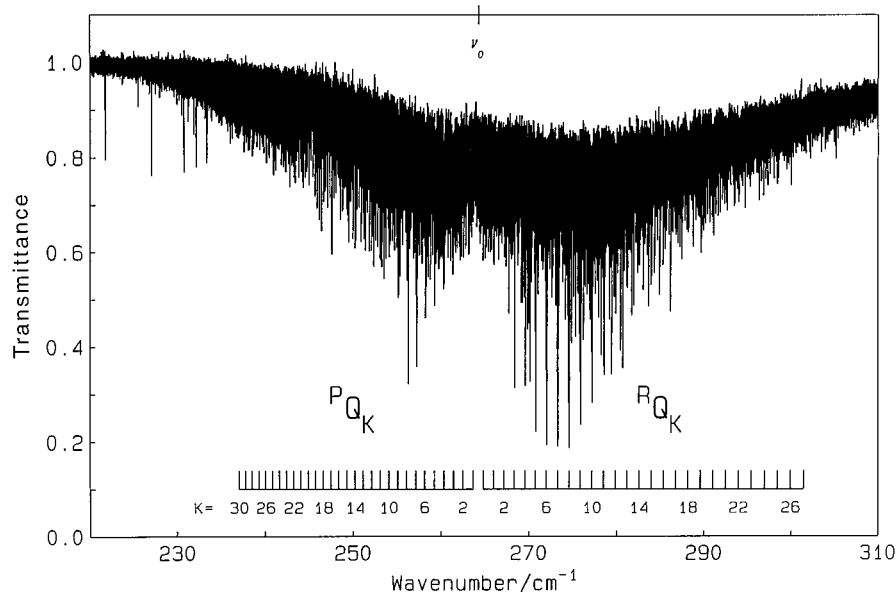


Figure 1. Overall appearance of the predominately B-type band of 1,2-difluoroethane- d_4 centered at 264 cm^{-1} . Locations of Q branches of subbands are designated with two combs.

CCF bending mode. This band is centered at 284.260 cm^{-1} for the normal isotopic species and is principally B-type in character. The B-type component of this band, which also has a weaker A-type component, has been fully analyzed and recently reported.¹⁶ The analysis of the corresponding B-type bands of the $^{13}\text{C}_2$ and d_4 isotopomers and the experimental determination of the structure of DFEA are the focus of this present report.

For the isotopic studies, the $^{13}\text{C}_2$ and d_4 isotopomers of DFEA had to be synthesized for the first time. These species were prepared by the reaction of AgF_2 with commercially available $^{13}\text{C}_2$ and d_4 isotopic modifications of 1,2-dibromoethane.

Experimental Section

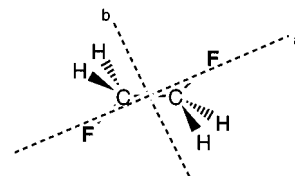
The reaction of AgF_2 with 1,2-dibromoethane to give DFEA has been described before.¹⁴ For the synthesis of the $^{13}\text{C}_2$ species 1,2-dibromoethane- $^{13}\text{C}_2$ (Cambridge Isotope Laboratory, Woburn, MA) was used, and for the synthesis of the d_4 species 1,2-dibromoethane- d_4 (CIL) was used. Preliminary identification of the isotopically substituted DFEAs, which were purified by preparative gas chromatography and dried by distillation over P_2O_5 , was by means of the reaction path, elution times, and low-resolution infrared spectra. The high-resolution study reported here confirms these identifications.

High-resolution infrared spectra were recorded at room temperature on a Bruker IFS 120 HR spectrometer in Giessen. Particulars of the instrument setup and calibration were as reported before.¹⁶ The resolution was a spectrometer-limited value of 0.0017 cm^{-1} (1/MOPD). For the spectrum of the $^{13}\text{C}_2$ species in the 279 cm^{-1} region, the sample pressure was 1.05 mbar, and the number of scans was 240. For the spectrum of the d_4 species in the 264 cm^{-1} region, the sample pressure was 1.4 mbar, and the number of scans was 300. For both spectra the overall path length was 13.12 m in the 0.82 m White cell.

A version of Dr. Arthur Maki's ASYMBD program was used to fit ground-state rotational constants to ground-state combination differences (GSCD) and to fit upper state rotational constants to spectral lines. The Giessen Loomis-Wood program facilitated assigning $^{\text{R}}\text{R}_K$ and $^{\text{P}}\text{P}_K$ series and processing large data sets when K_c -splitting was not too great.¹⁷

Results and Discussion

The d_4 and $^{13}\text{C}_2$ isotopomers of the anti rotamer of DFEA have the same C_{2h} symmetry as the normal species. As shown in the sketch, the axis for the smallest principal moment of inertia, I_a , lies in the plane of symmetry defined by the FCCF backbone and passes through the center of the molecule and near the two fluorine atoms. The axis for the intermediate



moment of inertia, I_b , also lies in the plane of symmetry. The c axis is perpendicular to this plane. The various isotopic species of the anti rotamer are near-prolate symmetric tops. For the normal species $\kappa = -0.98135$. For the d_4 species, $\kappa = -0.96584$, and for the $^{13}\text{C}_2$ species, $\kappa = -0.97980$. Of the 18 fundamentals nine are infrared active. The four modes of a_u symmetry, which involve atom displacements perpendicular to the plane of symmetry of the molecule, give bands of C-type in the gas-phase infrared spectrum. The five modes of b_u symmetry, which involve atom displacements that preserve the plane of symmetry, give bands of hybrid A/B shapes. The assignment of the vibrational fundamentals of the normal species, which is complete for modes of u symmetry but incomplete for modes of g symmetry, has been summarized.¹⁵ As yet, no attempt has been made to develop a full assignment of the fundamentals of either the gauche or anti rotamers of the d_4 and $^{13}\text{C}_2$ isotopomers.

Our interest for the present work is in the B-type component of the band due to the ν_{18} fundamental. This mode of b_u symmetry is mostly antisymmetric CCF bending. The frequency of this skeletal mode is rather insensitive to isotopic substitution. The wavenumber is 284 cm^{-1} for the normal species; it is 279 cm^{-1} for the $^{13}\text{C}_2$ and 264 cm^{-1} for the d_4 species. Thus, it is reasonable that the dominance of the B-type component of the band is preserved. This outcome is fortunate since only perpendicular bands give a good definition of all three principal rotational constants. As shown in the report on the high-

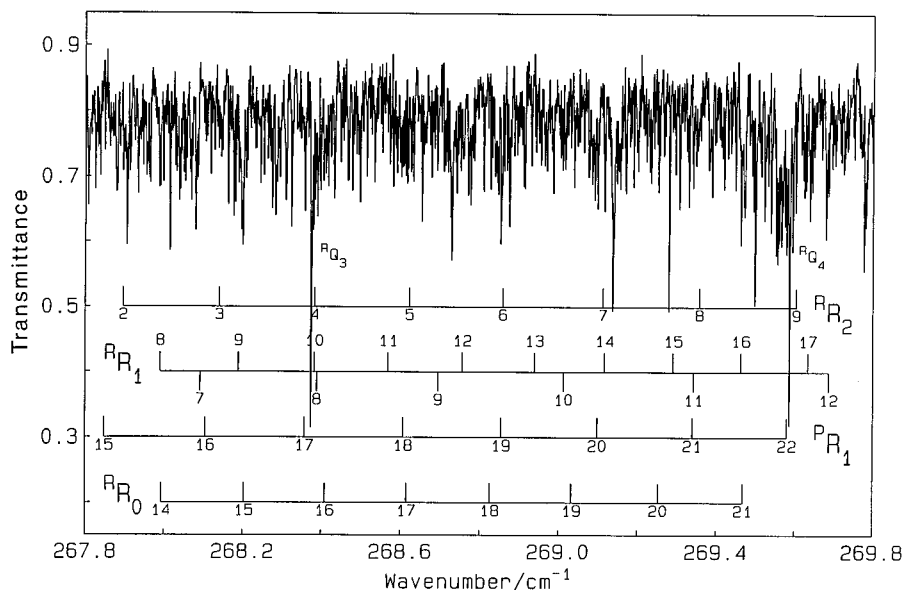


Figure 2. Detail of assignments of lines in subbands in the vicinity of RQ_3 and RQ_4 in the band for the d_4 species, including the start of the RR_2 series with high- K_c'' lines only.

resolution investigation of the normal species, this B-type band is the only candidate for a full analysis of the rotational structure as a basis for finding the structure of the anti rotamer.

For a B-type band the selection rules are $\Delta J = 0, \pm 1$, $\Delta K_a = \pm 1$, and $\Delta K_c = \pm 1, \pm 3$. Although intensities differ in these C_{2h} molecules for lines associated with different values of K_c due to nuclear spin statistics, the intensity differences for the d_4 and ${}^{13}C_2$ species are too small to assist in making assignments. The small difference in intensity for these molecules is a consequence of the sizable number of rotationally equivalent nuclei with spins.

The strategy that was used to assign the many subband series has been fully described.^{8,16} Suffice it to say here that the assignments began in the outer parts of the bands where prolate-symmetric-top theory applies. From GSCDs formed from P-branch ($K_a'' + 2$) and R-branch series (K_a''), ground-state (GS) rotational constants were refit as the number of series assigned grew. When the splitting of series due to differences in K_c indices became apparent, assignments in the P branch and computed GSCDs helped predict corresponding R-branch series, in which the splitting started at lower J values. Upper state (US) rotational constants were also fit to observed lines and to fixed, but updated GS constants in the growing data set. From the existing GS and US constants, lines in series progressively closer to the center of the band were predicted. These predictions guided assignments in this congested and complicated region. A Watson-type rotational Hamiltonian was employed in the A reduction and the F' representation as given before.¹⁴

Analysis of the B-Type Band near 264 cm^{-1} in the Spectrum of the d_4 Species. The overall appearance of the B-type band of the d_4 species centered at 264.257 cm^{-1} is shown in Figure 1. The assignments of the Q branches of the subbands are designated with the two combs. R-branch subband series were assigned from $K_a'' = 27$ to the band center. As an example, Figure 2 shows the detailed assignments of R-branch series in the vicinity of RQ_3 and RQ_4 . Splitting associated with different K_c'' values in R-branch series was first seen in the $K_a'' = 7$ series at $J'' = 45$. An example of this splitting is apparent for the RR_1 series in Figure 2. The splitting in the RR_2 series which begins at $J'' = 4$ is not shown in Figure 2. Only the lines associated with the higher K_c'' values are shown. The PR_1 and RR_0 series are unsplit. P-branch subband series

TABLE 1: Rotational Constants for the Anti Rotamer of 1,2-Difluoroethane- d_4

parameter	ground state ^a	ν_{18} vibrational state ^{a,b}
A	0.690 217 4 (17)	0.698 279 26 (94)
B	0.125 292 06 (50)	0.125 431 80 (99)
C	0.115 474 01 (37)	0.115 401 84 (41)
κ^c	-0.965 835	-0.965 585
$\Delta K \times 10^6$	1.1895 (38)	1.6365 (79)
$\Delta_{JK} \times 10^8$	-4.30 (17)	-3.857 (46)
$\Delta_J \times 10^8$	2.421 (14)	2.4530 (26)
$H_K \times 10^{11}$	1.71 (27)	-18.0 (17)
$H_{JK} \times 10^{12}$	-2.94 (38)	-3.92 (14)
$\delta_K \times 10^7$	-1.33 (11)	0.408 (41)
$\delta_J \times 10^{10}$	5.18 (68)	6.88 (13)
ν_0		264.256 828 (24)
std. dev.	0.000 46	0.000 45
no. lines fit ^d	983	1897
max. K_a'	29	18

^a In units of cm^{-1} ; uncertainties in last two numbers are given in parentheses. ^b Ground-state constants were held fixed while upper-state constants were being fitted. ^c Unitless. ^d Number of GSCDs or lines used in the fitting.

were assigned from $K_a'' = 29$ to the band center. Splitting associated with different K_c'' values in P-branch series begins in the $K_a'' = 8$ series at $J'' = 45$ in accord with the onset of splitting in R-branch series. A number of Q branches were also analyzed. In addition to the PQ_1 and RQ_0 branches in the band center, PQ_4 , PQ_3 , PQ_2 , RQ_1 , RQ_2 , RQ_3 , and RQ_4 branches were analyzed. A total of 2333 lines were assigned in the B-type component of the band. From these lines 983 nonredundant GSCDs were computed and fit with a standard deviation of 0.000 46 cm^{-1} .

Table 1 gives the GS rotational constants that were fit to the GSCDs for the d_4 species. These GS constants are slightly different ($\leq 0.000 32\%$) from the values previously reported due some tightening of the data set.¹⁵ Table 1 also gives the rotational constants for the first excited state of the ν_{18} fundamental. The fitting of the lines to the Hamiltonian for the US was broken off at $K_a' = 18$ because of the onset of a perturbation at $K_a' = 19$. With the mild exception of H_K the centrifugal distortion constants for the US are generally in good agreement with those in the GS. The large value of H_K may anticipate the perturbation that occurs at higher K_a values. Supplementary Table 1S gives all the GSCDs and the details of fitting the rotational Hamiltonian to the GS. Supplementary

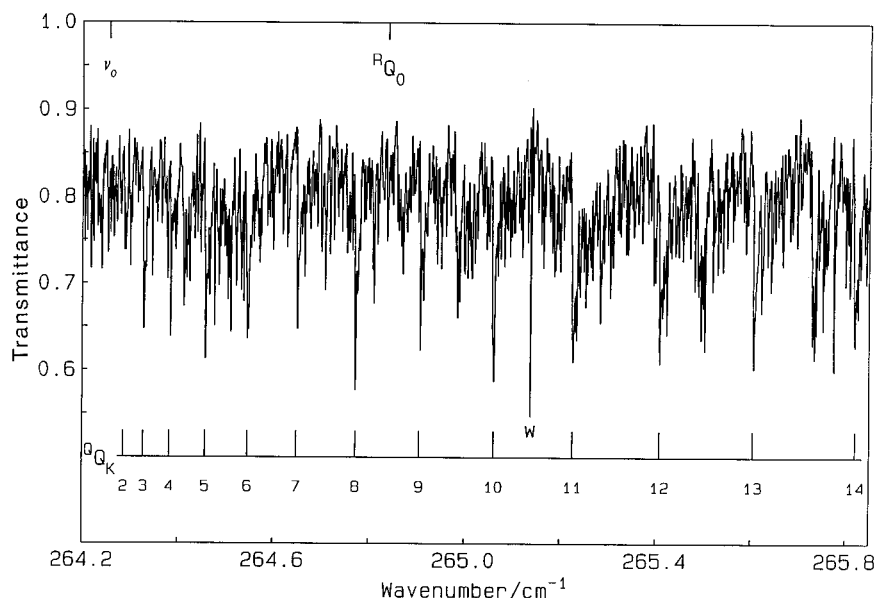


Figure 3. Q-branch origins of the A-type component near the center of the band for the d_4 species. ν_0 designates the band center, and RQ_0 the subband origin. The line marked with w is due to water.

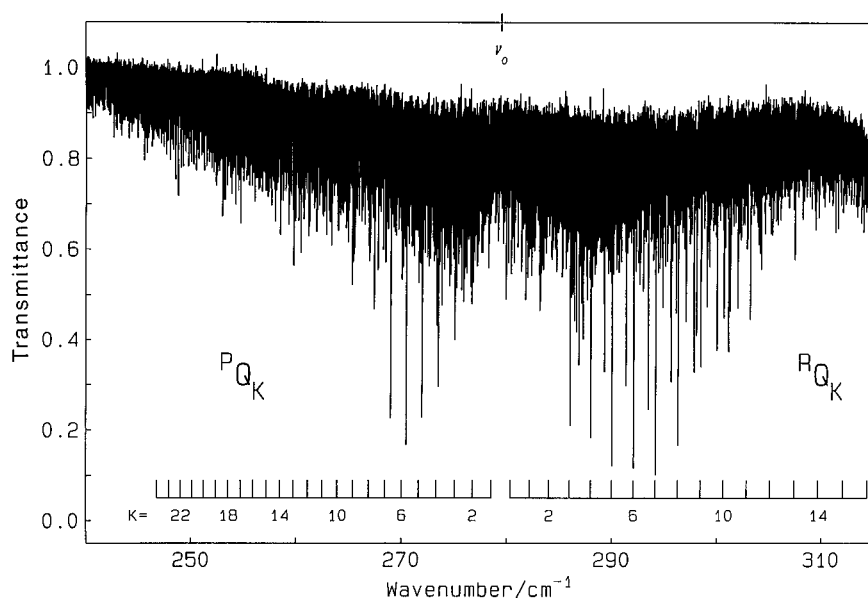


Figure 4. Overall appearance of the predominately B-type band of 1,2-difluoroethane- $^{13}C_2$ at 279 cm^{-1} . Locations of Q branches of subbands are designated with the two combs.

Table 2S gives the spectral lines that were used to fit to the US rotational Hamiltonian. Supplementary Table 3S contains the lines with $K_a' \geq 18$ that were not fit to the US Hamiltonian because of the perturbation. These additional lines were used to compute GSCDs.

Several characteristics of the assignment of the B-type band are notable. One of these features is that the lines in the ${}^R R_0$ and ${}^P R_1$ series coincide and the lines in the ${}^P P_1$ and ${}^R P_0$ series coincide as J increases. Figure 2 shows the lines in the ${}^P R_1$ series catching up with the lines of the same J'' in the ${}^R R_0$ series. The two series coalesce at $J'' = 42$. This coinciding of lines in the two subbands is consistent with B-type selection rules and the theory of asymmetric rotor energy levels as first described and diagrammed by Dieke and Kistiakowsky.¹⁸ Beyond $J'' = 41$, only the ${}^R P_0$ and ${}^R R_0$ lines were retained in the data set. A second characteristic of the overall assignment is the prediction of lines in the A-type component of this band from rotational constants fit to the B-type component. When the transitions in the A-type component were calculated from the rotational constants in Table 1, the locations of the ${}^Q Q_K$ clusters near the

band center were predicted correctly. This result is shown in Figure 3. The rather wide spacing of these features is a consequence of the significant increase in the A rotational constant by about 1% on going from the GS to the US. The rather wide spacing of Q-branch clusters for the A-type band prevents recognition of this component in the survey of the band shown in Figure 1. A third characteristic of the overall assignment is its consistency with the locations of local band heads. In accord with the fitting of the US constants, band heads were found in ${}^R Q_1(\text{low-}K_c)$ at $J'' = 15$, in ${}^P Q_2(\text{low-}K_c)$ at $J'' = 15$, and in ${}^P Q_4(\text{high-}K_c)$ at $J'' = 20$.¹⁹ These three characteristics of the assignment for the d_4 species were also found earlier in the assignment of corresponding band of the normal species of DFEA.¹⁶

Analysis of the B-Type Band near 279 cm^{-1} in the Spectrum of the $^{13}C_2$ Species. Figure 4 shows the predominately B-type band of the $^{13}C_2$ isotopomer of DFEA centered at 279.410 cm^{-1} . The locations of Q branches of subbands are designated with separate combs for the P and R branches. Subbands were assigned in the P branch to $K_a'' = 24$. In the R

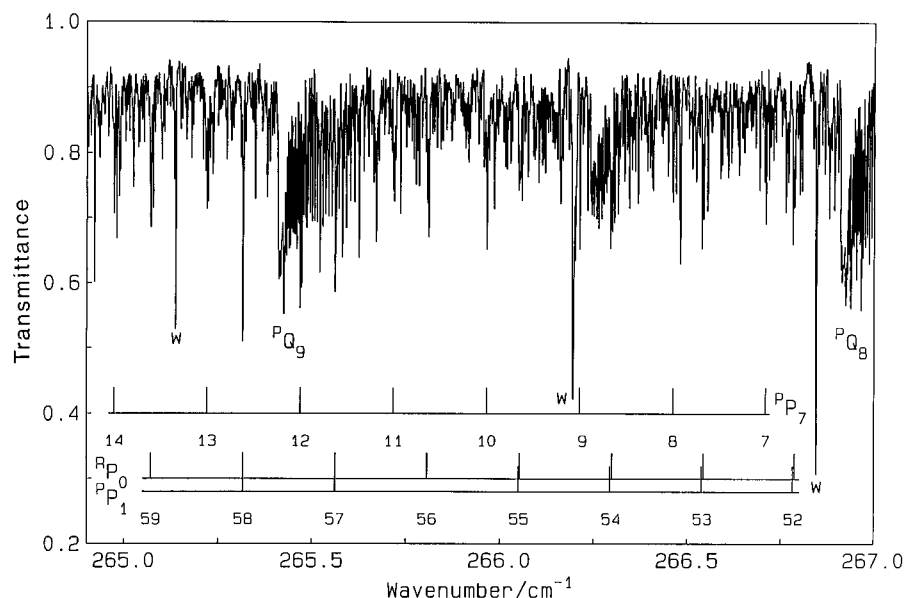


Figure 5. Detail of assignments of lines in subbands in the vicinity of PQ_8 and PQ_9 in the band for the ${}^{13}C_2$ species, including the start of the PP_7 series and the coalescence of the RP_0 and PP_1 lines at $J'' = 58$. Lines marked *w* are due to water.

branch, subband assignments were limited to a maximum of $K_a'' = 18$ due to interference from a rather structureless band of an unidentified impurity centered at 331 cm^{-1} . (The A-type impurity band with a PR separation of 16 cm^{-1} was not in the synthesized material.) A number of Q branches were also analyzed. In addition to the PQ_1 and RQ_0 branches in the band center, PQ_6 , PQ_5 , PQ_4 , PQ_3 , PQ_2 , RQ_1 , RQ_2 , RQ_3 , RQ_4 , and RQ_5 branches were assigned.

Figure 5 depicts the P branch in detail in the vicinity of the PQ_8 and PQ_9 . Lines for the PP_7 series begin in this region. Also, the coalescence of the RP_0 and PP_1 lines at $J'' = 58$ is apparent. A corresponding coalescence of PR_1 and RR_0 lines occurs in the R branch as required by asymmetric rotor theory. K_c splitting was first seen at $K_a'' = 6$ and $J'' = 44$. The onset of observable splitting occurs at a lower K_a'' value than for the d_4 species as is appropriate for the ${}^{13}C_2$ species being more nearly a symmetric top.

For the overall B-type component of the band, 2342 lines were assigned. From these assignments 1033 GSCDs were derived and used to fit the rotational constants of the GS Hamiltonian as summarized in Table 2. The standard deviation in the GS fitting was a satisfactory 0.00042 cm^{-1} . Supplementary Table 4S gives all of the GSCDs used and the details of fitting the GS rotational constants. These GS constants are slightly different ($\leq 0.00021\%$) from the values previously reported.¹⁵ Table 2 also gives the rotational constants for the first excited state of the ν_{18} fundamental. For fitting the US rotational constants to the Hamiltonian, assigned lines were limited to $K_a' \leq 14$ due to a perturbation at higher K_a' values. The lines used in the fitting and the details of the fitting of US constants are in supplementary Table 5S. In general, as seen in Table 2, the centrifugal distortion constants are similar for the US and GS. Those lines not used in the US fitting but used, in part, in computing GSCDs are in supplementary Table 6S. These lines extend from $K_a'' = 14$ to 18 in the R branch and $K_a'' = 16$ to 24 in the P branch.

Special characteristics of the assignment of the lines for the ${}^{13}C_2$ species were similar to those of the normal and d_4 species. First, as already noted, the PP_1 and RP_0 series become coincident as do the PR_1 and RR_0 series at $J'' = 58$. Second, the series of rather widely separated QQ_K clusters for the A-type component were found in the band center as accurately predicted from the

TABLE 2: Rotational Constants for the Anti Rotamer of 1,2-Difluoroethane- ${}^{13}C_2$

	ground state ^a	ν_{18} vibrational state ^{a,b}
<i>A</i>	1.022 408 4 (15)	1.042 241 4 (14)
<i>B</i>	0.128 806 12 (51)	0.128 942 28 (13)
<i>C</i>	0.119 688 80 (34)	0.119 610 42 (10)
κ^c	-0.979 800	-0.979 771
$\Delta_K \times 10^6$	3.7096 (27)	6.459 (20)
$\Delta_{JK} \times 10^8$	-8.85 (18)	-9.71 (10)
$\Delta_J \times 10^8$	2.529 (15)	2.7030 (57)
$H_K \times 10^{10}$	0.0	-8.47 (75)
$H_{KJ} \times 10^{11}$	0.0	-4.62 (53)
$H_{JK} \times 10^{12}$	3.61 (45)	2.06 (26)
$\delta_K \times 10^6$	-1.699 (24)	-0.961 (24)
$\delta_J \times 10^{10}$	1.55 (73)	9.28 (24)
ν_0		279.409 844 (25)
std. dev.	0.000 42	0.000 42
no. lines ^d	1033	1960
max. K_a'	20	14

^a In units of cm^{-1} ; uncertainties in last two numbers are given in parentheses. ^b Ground-state constants were held fixed while upper-state constants were being fitted. ^c Unitless. ^d Number of GSCDs or lines used in the fitting.

rotational constants fit to the B-type component. Third, a number of local bandheads for subband series were found. They were for ${}^PQ_5(\text{high-}K_c)$, ${}^PQ_4(\text{high-}K_c)$, ${}^PQ_3(\text{low-}K_c)$, ${}^PQ_2(\text{low-}K_c)$, ${}^RP_1(\text{high-}K_c)$, ${}^RR_2(\text{low-}K_c)$, ${}^RQ_1(\text{low-}K_c)$, ${}^RQ_2(\text{low-}K_c)$, and ${}^RQ_4(\text{high-}K_c)$.

Geometric Parameters for the Anti Rotamer of 1,2-Difluoroethane. Table 3 gives the moments of inertia for the GS of DFEA that were derived from the *A*, *B*, and *C* rotational constants reported previously for the normal species¹⁵ and listed in Tables 1 and 2 for the d_4 and ${}^{13}C_2$ species, respectively. The values for the ${}^{13}C_2$ and d_4 species differ slightly from those that we reported in the preliminary communication.¹⁴

The moments of inertia in Table 3 were used in two ways to obtain geometric parameters for the anti rotamer of DFEA. They were used to obtain Cartesian coordinates for the carbon and hydrogen atoms by the substitution (r_s) method. Then, with the resulting *geometric parameters* for the carbon and hydrogen atoms held fixed, Cartesian coordinates were found for the fluorine atoms and slightly revised Cartesian coordinates were found for the carbon and hydrogen atoms from fitting to the full set of moments of inertia.²⁰ This overall result is designated

TABLE 3: Principal Moments of Inertia for the Anti Rotamer of 1,2-Difluoroethane and Its Isotopomers (I 's in u \AA^2)

	I_a	I_b	I_c
$\text{H}_2\text{FC}-\text{CFH}_2^a$	15.942 75	130.285 08	139.717 80
$\text{H}_2\text{F}^{13}\text{C}-^{13}\text{CFH}_2$	16.488 16	130.876 01	140.845 52
$\text{D}_2\text{FC}-\text{CFD}_2$	24.423 66	134.546 69	145.986 37

^a From ref 15. All other values from the present work.

TABLE 4: Cartesian Coordinates for the Anti Rotamer of 1,2-Difluoroethane (in \AA)

atom	principal axis system		
	a	b	c
r_s carbon ($^{13}\text{C}_2$) ^a	± 0.5339	± 0.5263	0.0
r_s hydrogen (d_4) ^a	± 0.4808	± 1.1516	± 0.8968
r fluorine ^b	± 1.7718	∓ 0.1333	0.0
r_0 carbon	± 0.5373	± 0.5278	0.0
r_0 hydrogen	± 0.4913	± 1.1470	± 0.8981
r_0 fluorine	± 1.7707	∓ 0.1349	0.0

^a Direct substitution coordinates for carbon and hydrogen are $a = -0.5394$, $b = -0.5206$, $c = 0.0$ and $a = 0.4928$, $b = -1.1465$, $c = 0.8968$, respectively. ^b With carbon and hydrogen atoms held at substitution coordinates and I 's of the parent species fit, fluorine coordinates are $a = 1.7710$, $b = 0.1347$, and $c = 0.0$. When P 's are fit, fluorine coordinates are $a = 1.7702$, $b = 0.1345$, and $c = 0.0$.

r_s/r_0 . For the second, purely r_0 analysis Cartesian coordinates were found for all three types of atoms by a simultaneous fitting to the full set of moments of inertia.

For the r_s coordinates of the carbon atoms the appropriate expressions for 2-fold substitution with ^{13}C in the anti structure were as given in Gordy and Cook.²¹ Corresponding expressions for the 4-fold substitution of hydrogen atoms were not available in standard sources. We derived these expressions from the general theory of multiple substitution as given by Chutjian.²² The expressions are

$$a^2 = [(I'_c - I_c)/(4\Delta m)] - b^2$$

$$b^2 = [I_a(I_a - I'_a - I'_b) + I'_a I'_b] / [4\Delta m(I_b - I_a)] - c^2(-I_a + I_b + I'_c - I_c)/(I_b - I_a) - 4\Delta m c^4/(I_b - I_a)$$

$$c^2 = [(I'_a - I_a) + (I'_b - I_b) - (I'_c - I_c)]/8\Delta m$$

For the anti rotamer of DFEA Table 4 gives the adjusted Cartesian coordinates of carbon and hydrogen atoms and the associated coordinates of the fluorine atoms as obtained from

the r_s/r_0 analysis. These values are the ones labeled r_s and r in the first three rows of Table 4. The initial, direct r_s Cartesian coordinates for the carbon and hydrogen atoms are given in a footnote to Table 4. This table also gives the r_0 coordinates for all three atom types as obtained from a global fitting to the three sets of moments of inertia. The University of Michigan adaptation of Professor Richard Schwendeman's program was used for the fittings.

Table 5 provides a comparison of experimental and theoretical geometric parameters of the gauche and anti rotamers of DFEA. The set of experimental values for the gauche rotamer is from the microwave investigation of Takeo, Matsumura, and Morino.¹¹ These workers used an extensive set of isotopomers in their investigation. The two sets of experimental parameters for the anti rotamer are from the present study. The first set, labeled "anti r_s/r_0 ", was obtained as described above. The uncertainties given with the r_s/r_0 values are those found by the Costain method. The second set, labeled "anti r_0 ", comes from Cartesian coordinates found in the global fitting. The accompanying uncertainties are those computed in the least-squares fitting. Some of the r_0 values differ slightly from those reported previously by us due to small changes in refitting the rotational constants.¹⁵ Although the agreement between the two methods of extracting the geometric parameters is generally good, two differences are a bit large. These differences are for the CC bond length and the HCH bond angle. A likely reason for these differences is the cumulative effect of CH/CD anharmonicity in using the d_4 species. The r_0 values are the preferred geometric parameters for the anti rotamer of DFEA for comparison with those for the gauche rotamer of DFEA which were obtained by the same methodology.

As seen in Table 5, the principal adjustments in bond parameters that occur in going from the gauche to the anti rotamer of DFEA are in the CCF and CCH bond angles. The CCF bond angle decreases by 3.2° . One CCH bond angle, the one anti to the CF bond on the other carbon atom, changes negligibly, whereas the other CCH bond angle increases by 3.1° . Thus, in the gauche rotamer the CFH moieties which include the gauche CH bonds rotate approximately as a whole in the adjustment between the two rotamers. Experimentally, the CC and CF bonds are somewhat longer in the anti rotamer with the difference being comparable to the sum of the uncertainties in the values for the two rotamers. In general, the differences between the gauche and anti rotamers of DFEA are similar to the differences between the cis and trans isomers of 1,2-difluoroethylene.¹⁴ The one exception is that the CC bond length decreases in going from the cis to the trans isomer in 1,2-difluoroethylene.

TABLE 5: Experimental and Theoretical Geometric Parameters for the Gauche and Anti Rotamers of 1,2-Difluoroethane

	r_{CH}^a	r_{CC}^a	r_{CF}^a	α_{CCH}^b	α_{HCH}^b	α_{CCF}^b	α_{FCH}^b	method
				Experimental ^c				
gauche r_0	1.099(2) ^d	1.493(8)	1.390(3)	108.4(6) ^d	109.1(5)	110.6(5)	109.6(3) ^d	MW ^f
	1.093(5) ^e			111.3(6) ^e			107.8(6) ^e	
anti r_s/r_0 ^g	1.095(2)	1.499(4)	1.403(6)	111.5(2)	110.0(3)	107.4(5)	108.1(3)	IR ^h
anti r_0	1.092(1)	1.506(5)	1.400(4)	111.6(3)	110.7(1)	107.3(2)	107.8(3)	IR ^h
				Theoretical				
gauche r_c	1.093 ^d	1.500	1.385	109.4 ^d	109.5 ⁱ	111.0	108.1 ^j	calc ^k
	1.092 ^e			110.7 ^{e,i}			108.0 ^j	
anti r_c	1.091	1.514	1.387	110.9	109.5 ⁱ	108.4	108.5	calc ^k

^a Bond lengths in \AA . ^b Angles in degrees. ^c Uncertainties in last place in parentheses as reported in the microwave study in ref 11, as found in the least-squares fitting for the r_0 values, and as estimated by the Costain method for the r_s values. ^d For the CH bond gauche relative to the CF bond on the other carbon atom. ^e For the CH bond anti relative to the CF bond on the other carbon atom. ^f ref 11. ^g Different values obtained when substitution Cartesian coordinates are held fixed for the carbon and hydrogen atoms are $r_{\text{CF}} = 1.395(6)$ \AA , $\alpha_{\text{CCF}} = 108.0(5)$ and $\alpha_{\text{FCH}} = 107.8(3)$. ^h Present work. ⁱ Revised by authors, ref 9. ^j Computed from Cartesian coordinates supplied by the authors, ref 9. ^k Ref 9. As confirmed by the authors, the gauche and anti designations for CH bonds had to be reversed to agree with the choice in ref 1.

Table 5 also contains theoretical (r_e) values for the geometric parameters of the two rotamers of DFEA found by Muir and Baker in a recent ab initio investigation.⁹ Although the absolute values for the parameters of the individual rotamers differ some from those obtained by Durig and co-workers with a 6-311++G** basis set,^{2,23} the differences in parameters between the two rotamers are similar in the two sets of calculations. With the exception of the noticeable change in the CF bond length in the experimental results, the changes in the parameters between rotamers found in the experimental data are similar to those found in the ab initio calculations. Agreement with absolute values is also reasonably good given that the experimental values are for the ground state and the theoretical values are equilibrium ones.

For the energy difference between the two rotamers of DFEA, ab initio investigations give the correct sign even with RHF-level calculations if the basis set is sufficiently flexible. The value computed is about 0.84 kJ/mol.^{2,7,24} With higher levels of theory that include electron correlation, the anti-gauche energy difference is computed to be 2.5–3.3 kJ/mol,^{7,25} in excellent agreement with experiment.^{1,2} Although accommodating the “anomalous” bond parameters and energies in fluorocarbons is computationally challenging, these effects appear to be contained within high-level ab initio calculations. What is yet to emerge unambiguously from the ab initio work is a qualitative understanding of the unusual effects.

Many of the adjustments in geometric parameters between the gauche and anti rotamers of DFEA conform to Wiberg's qualitative interpretation.⁶ The larger CCF bond angle in the gauche rotamer of DFEA in comparison with the anti rotamer is as expected for the greater CF bond repulsion in this rotamer, notwithstanding the lower electronic energy of the gauche rotamer. For the isomers of 1,2-difluoroethylene an analogous relationship exists for the CCF bond angle. Also consistent with repulsion of CF bond moments in the gauche rotamer, the FCCF dihedral angle of 71.0(3)° in this rotamer is appreciably larger than the default value of 60°. The sympathetic adjustment in one CCH bond angle is also consistent with the Wiberg model. The increased CC bond length in the anti rotamer is consistent with the bond weakening compared to the gauche rotamer. Taking into account the estimated uncertainties for the CC bond in the microwave-derived value for the gauche rotamer and in the present value for the anti rotamer, we must be cautious about this difference between experiment and theory. The apparently longer CF bond in the anti rotamer does not conform to the Wiberg model, since the effect of rehybridization should be common to the two rotamers. In addition, the same, bent bond explanation applies to the isomers of 1,2-difluoroethylene as to the rotamers of DFEA. Thus, the shortening of the CC bond by about 0.01 Å in going from the cis to the trans isomer is not consistent with this model. The ab initio calculations of Muir and Baker show a negligible change in the CC bond length between the two ethylene isomers,⁹ as do earlier ab initio calculations.⁸

The qualitative valence bond analysis of Epiotis not only accounts for the CCF and CCH angle changes between the gauche and anti rotamers of DFEA but also anticipates the CC and CF bond length increases in going to the anti rotamer.¹⁰ In contrast to other analyses, Epiotis anticipates an increase in CF bond length between the gauche and anti rotamers but a decrease in the CC bond length in going from cis to trans 1,2-difluoroethylene as is found experimentally. He argues that the key reasons differ for the gauche and cis effects.

It seems likely that the newly acquired experimental parameters for nonpolar partners in the interesting 1,2-difluoroethane

rotamers and 1,2-difluoroethylenes isomers will attract renewed efforts with high-level ab initio calculations and qualitative interpretations to account for the gauche and cis effects.

Acknowledgment. We are grateful to Baonian Hu and Gibran el-Sulayman for assistance with the synthetic work. We also benefited from discussions with Professor Robert L. Kuczkowski about the structure fitting. This research was supported by National Science Foundation Grant CHE-9207156. The high-resolution spectroscopy was done while N.C.C. was in residence at Justus-Liebig-University in Giessen and was supported by a grant from the Deutscher Akademischer Austauschdienst.

Supporting Information Available: Table 1S contains the GSCDs and the fitting of GS rotational constants for the d₄ species of TFEA. Table 2S contains most of the lines assigned in the B-type band of TFEA-d₄ and the fitting of the US rotational constants. Table 3S supplements Table 2S by giving the higher K_a lines of the B-type band of TFEA-d₄ in the perturbed region. Table 4S contains the GSCDs and the fitting of the GS constants for TFEA-¹³C₂. Table 5S has most of the lines assigned in the B-type band of TFEA-¹³C₂ and the fitting of the US constants. Table 6S supplements Table 5S by giving the higher K_a lines of the B-type band of TFEA-¹³C₂ in the perturbed region (40 pages). See any current masthead page for ordering information and Internet access.

References and Notes

- (1) Huber-Wälchli, P.; Günthard, H. *Spectrochim. Acta* **1981**, *37A*, 285.
- (2) Durig, J. R.; Liu, J.; Little, T. S.; Kalasinsky, V. F. *J. Phys. Chem.* **1992**, *96*, 8224.
- (3) Wolfe, S. *Acc. Chem. Res.* **1972**, *5*, 102.
- (4) Connor, T. M.; McLauchlan, K. A. *J. Phys. Chem.* **1965**, *69*, 1888.
- (5) Craig, N. C.; Piper, L. G.; Wheeler, V. L. *J. Phys. Chem.* **1971**, *75*, 1453.
- (6) Wiberg, K. B. *Acc. Chem. Res.* **1996**, *29*, 229.
- (7) Dixon, D. A.; Smart, B. E. *J. Phys. Chem.* **1988**, *92*, 2729.
- (8) Craig, N. C.; Brandon, D. W.; Stone, S. C.; Lafferty, W. J. *J. Phys. Chem.* **1992**, *96*, 1598.
- (9) Muir, M.; Baker, J. *Mol. Phys.* **1996**, *89*, 211.
- (10) Epiotis, N. D. *Deciphering the Chemical Code. Bonding across the Periodic Table*; VCH Publishers: New York, 1996; Chapter 11.
- (11) Takeo, H.; Matsumura, C.; Morino, Y. *J. Chem. Phys.* **1986**, *84*, 4205.
- (12) Van Schaick, E. J. M.; Geise, H. J.; Mijlhoff, F. C.; Renes, G. J. *Mol. Struct.* **1973**, *16*, 23.
- (13) Friesen, D.; Hedberg, K. J. *Am. Chem. Soc.* **1980**, *102*, 3987.
- (14) Craig, N. C.; Abiog, O. P.; Hu, B.; Stone, S. C.; Lafferty, W. J.; Xu, L.-H. *J. Phys. Chem.* **1996**, *100*, 5310.
- (15) Craig, N. C.; Chen, A.; Suh, K. H.; Klee, S.; Mellau, G. C.; Winnewisser, B. P.; Winnewisser, M. J. *Am. Chem. Soc.* **1997**, *119*, 4789.
- (16) Craig, N. C.; Klee, S.; Mellau, G. C.; Winnewisser, B. P.; Winnewisser, M. J. *J. Phys. Chem.* **1996**, *100*, 15049.
- (17) Winnewisser, B. P.; Reinstädler, J.; Yamada, K. M. T.; Behrend, J. *J. Mol. Spectrosc.* **1989**, *136*, 12.
- (18) Dieke, G. H.; Kistiakowsky, G. B. *Phys. Rev.* **1934**, *45*, 4.
- (19) High-K_c refers to high-K_c' = low-K_c' + 1 associated with a given J'' for a split K_a' series.
- (20) This mixed r_s/r₀ method was also used in finding one of the two structures for trans-1,2-difluoroethylene. The Cartesian coordinates for carbon and hydrogen atoms given in Table 5 in ref 14 are the direct r_s values. The slightly modified values obtained when fitting the fluorine coordinates are a = 0.5132, b = 0.4121, and c = 0.0 for a carbon atom and a = 0.4698, b = 1.4923, and c = 0.0 for a hydrogen atom.
- (21) Gordy, W.; Cook, R. L. *Microwave Molecular Spectra*, 3rd ed.; Wiley-Interscience: New York, 1984.
- (22) Chutjian, A. *J. Mol. Spectrosc.* **1964**, *14*, 361.
- (23) The geometric parameters reported by Durig et al., ref 2, are very similar to those given by Dixon and Smart, ref 7, and by Wiberg and Murcko, ref 23.
- (24) Wiberg, K. B.; Murcko, M. A. *J. Phys. Chem.* **1987**, *91*, 3616.
- (25) Wiberg, K. B.; Murcko, M. A.; Laidig, K. E.; MacDougall, P. J. *J. Phys. Chem.* **1990**, *94*, 6956.